ELSEVIER

Journal of Nuclear Materials 250 (1997) 1–12

journal of nuclear materials

Critical evaluation of the thermal properties of ThO_2 and $Th_{1-y}U_yO_2$ and a survey of the literature data on $Th_{1-y}Pu_yO_2$

K. Bakker, E.H.P. Cordfunke, R.J.M. Konings *, R.P.C. Schram

Netherlands Energy Research Foundation ECN, P.O. Box 1, 1755 ZG Petten, The Netherlands

Received 5 May 1997; accepted 22 July 1997

Abstract

The thermal properties of ThO_2 and $Th_{1-y}U_yO_2$ are critically assessed. These properties include melting point, heat capacity, enthalpy of formation, oxygen potential, thermal conductivity and linear thermal expansion. The literature survey of the thermal properties of $Th_{1-y}Pu_yO_2$ shows a limited amount of data, as a result a critical evaluation is not possible. In addition, the phase diagrams of the binary systems ThO_2–UO_2 and ThO_2–PuO_2 are discussed. © 1997 Elsevier Science B.V.

1. Introduction

The major part of the nuclear power is generated in reactors which use uranium as fuel, where ^{235}U is the fissile material and ^{238}U is the fertile matrix. From an environmental point of view is the production of transuranium elements through neutron capture in ^{238}U a major disadvantage of the use of uranium fuel. These elements, in particular plutonium, neptunium and americium, contribute significantly to the long-term radiotoxicity of the high-level waste. Presently, partitioning and transmutation of the above mentioned transuranium elements is attracting much attention as it might be a means to achieve a considerable reduction of the radiotoxicity of the waste from nuclear power production.

A different approach to this waste problem is the use of thorium-based fuel, as reactors operated in a thorium fuel cycle will produce less transuranium elements per unit of fission energy. However, the alpha-toxicity of the waste from thorium-fueled reactors is still above the level of the ore of which the fuel is fabricated, as long-lived uranium isotopes (^{233}U, ^{234}U) are formed in significant amounts during irradiation. Because natural thorium, ^{232}Th, is not a fissile nuclide, an external start-up material has to be added to a thorium-based fuel. This can be ^{233}U obtained from reprocessing of thorium fuel, ^{235}U, or plutonium from reprocessing of LWR fuel.

The behaviour of nuclear fuel during irradiation is highly dependent on the physico–chemical properties of the fuel material, and their variation with temperature and burn-up. For example, the fuel temperature is determined, amongst others, by the thermal conductivity of the fuel material. A poor thermal conductivity leads to a large temperature gradient across the fuel pellet and a high central temperature of the fuel pin. The physico–chemical properties of the fuel are not constant during the irradiation period in the reactor, but vary with the burn-up. Some fission products will dissolve in the fuel matrix, but others can form gas-bubbles or precipitates, depending on the oxygen potential. The formation of gas bubbles and precipitates may lead to swelling of the fuel, and, in the worst case, failure of the fuel pin thus affecting the safety of the reactor.

The properties of thoria-based fuels have been studied extensively in the past, especially in the sixties, and have often not been published in easily accessible literature sources. As part of our study on nuclear fuels with low plutonium production a critical review of the thermal properties of ThO_2 as well as the ThO_2–UO_2 and ThO_2–PuO_2 solid solutions has been made and the results are reported here. Since very little is known on the influence of burnup on the properties of thoria-based fuels, this problem is not treated here.

* Corresponding author. Fax: +31-224 563 608; e-mail: konings@ecn.nl.

PII S0022-3115(97)00241-9

2. ThO_2

2.1. Enthalpy of formation

The enthalpy of formation of thorium dioxide is a CODATA Key Value [1]:

$$\Delta_f H^0(298.15\ \mathrm{K}) = -(1226.4 \pm 3.5)\ \mathrm{kJ\ mol^{-1}}. \quad (1)$$

This value is based on the enthalpy-of-combustion measurements by Huber et al. [2]. Earlier measurements by Roth and Becker [3] gave $-(1226 \pm 5)$ kJ mol^{-1}, which is in good agreement with the selected value.

2.2. Heat capacity

The low-temperature heat capacity of ThO_2 has been measured by Osborne and Westrum [4]. These measurements were used in the CODATA Key Values selection [1] to obtain

$$S^0(298.15\ \mathrm{K}) = (65.23 \pm 0.20)\ \mathrm{J\ K^{-1}\ mol^{-1}}. \quad (2)$$

The high-temperature enthalpy increment of ThO_2 has been measured by Jaeger and Veensta [5], Southard [6], Hoch and Johnston [7], Victor and Douglas [8], Springer et al. [9,10] and Fischer et al. [11]. The data cover the temperature range 500 to 3400 K, as shown in Fig. 1. Up to 2500 K the results are in fair agreement, except in the low-temperature region where the data of Victor and Douglas and of Springer et al. [1] deviate significantly due to small inaccuracies in temperature or enthalpy that become prominent close to 298.15 K when using this function.

Above 2500 K, ThO_2 exhibits an excess enthalpy, like many high-melting refractory oxides (e.g., UO_2, PuO_2 and ZrO_2). Fischer et al. suggested that this effect is due to a phase transformation and this possibility was studied in detail by Ronchi and Hiernaut [12] using a thermal arrest technique. From their results, Ronchi and Hiernaut concluded that a λ-type pre-melting transition occurs at 3090 K, which was attributed to order–disorder anion displacements in the oxygen sublattice (Frenkel defects).

For the recommended values the results of Southard [6], Hoch and Johnston [7] and Fischer et al. [11] have been combined and fitted to the equation (298.15–3500 K)

$$\{H^0(T) - H^0(298.15\ \mathrm{K})\}/\mathrm{J\ mol^{-1}} = 55.9620(T/\mathrm{K}) + 25.62895 \times 10^{-3}(T/\mathrm{K})^2 - 12.2674 \times 10^{-6}(T/\mathrm{K})^3 + 2.30613 \times 10^{-9}(T/\mathrm{K})^4 + 5.740310 \times 10^5(T/\mathrm{K})^{-1} - 20581.7 \quad (3)$$

constrained to $C_p^0(298.15\ \mathrm{K}) = 61.76\ \mathrm{J\ K^{-1}\ mol^{-1}}$, as derived from the low-temperature heat capacity measurements by Osborne and Westum [4], and $\{H^0(T) - H^0(298.15\ \mathrm{K})\} = 0\ \mathrm{J\ mol^{-1}}$ at 298.15 K. The C_p^0 derived from this function, of course, does not reproduce the heat capacity data by Ronchi and Hiernaut [12] around the λ-transition, which show a maximum value of 600 J K^{-1} mol^{-1}.

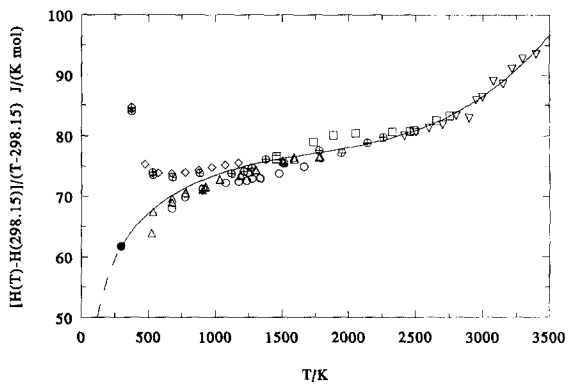

Fig. 1. The reduced enthalpy increment of ThO_2; ○, Jaeger and Veenstra; △, Southard; □, Hoch and Johnston; ◇, Victor and Douglas; ▽, Fischer et al.; ⊕, Springer et al.; ●, Osborne and Westrum.

No experimental data are available for liquid thorium dioxide. Fink et al. [13] estimated $C_p^0(\mathrm{liq}) = 61.76\ \mathrm{J\ K^{-1}\ mol^{-1}}$ for the heat capacity of the liquid.

2.3. Melting point

The melting point of ThO_2 has been measured by several authors, as summarized in Table 1. The reported values vary from 3323 to 3808 K, but the more recent ones agree about a melting point around 3600 K. We here consider the value measured by Ronchi and Hiernaut [12], (3651 ± 17) K, as the most accurate one as it was determined on a well-defined sample (O/Th ratio = 2.00) and with a well-defined technique.

2.4. Vapour pressure

The vapour pressure of ThO_2 has been measured by several authors [14–19] using indirect measurement tech-

Table 1
The melting point of ThO_2

T_{fus} (K)	Authors	Year
3323	Ruff et al. [88]	1929
3803	Wartenberg and Reusch [89]	1932
3323 ± 25	Geach and Harper [90]	1953
3573 ± 100	Lambertson et al. [46]	1953
3663 ± 100	Benz et al. [91]	1969
3573	Chikalle et al. [92]	1972
3651 ± 17	Ronchi and Hiernaut [12]	1996
3651 ± 17		selected value

[1] The data listed by Spinger et al. have been corrected for obvious typographical errors.

Table 2
The enthalpy of sublimation of ThO_2 at 298.15 K

$\Delta_{sub}H^0$ (kJ mol^{-1})		T (K)	Method [a]	Authors	Year
uncorrected	corrected [b]				
772.0		2060–2250	W	Shapiro [14]	1952
710.9 ± 3.0		2398–2676	K	Hoch and Johnston [15]	1954
765.6 ± 2.3		2268–2593	K	Darnell and McCollum [16]	1961
763.2 ± 2.0	770	2180–2871	K	Ackermann et al. [17]	1963
790.3 ± 4.2		2380–2900	T	Alexander et al. [18]	1967
759.0		2057–2421	M	Cears et al. [19]	1980
770 ± 10	selected value				

[a] K = Knudsen effusion, M = mass spectrometry, W = weight loss, T = Transpiration.
[b] See text.

niques such as Knudsen effusion or transpiration methods. In the interpretation of the results of these studies it was generally assumed that the vapour above ThO_2(cr) consist entirely of ThO_2 molecules, which is not true as a mass-spectrometric study also reveals the presence of ThO(g) and O(g). This was discussed in detail by Ackermann and Rauh [20] and Belov and Semenov [21].

Ackermann and Rauh corrected the total vapour pressure from their earlier Knudsen study (Ackermann et al. [17]) to a partial pressure of ThO_2(g). This was done by calculating the partial pressures of ThO(g) and O(g) over stoichiometric ThO_2 (2400–2800) K:

$$\log(p_{ThO}/p^0) = -36\,860(T/K)^{-1} + 8.15 \quad (4)$$

and

$$\log(p_O/p^0) = -36\,860(T/K)^{-1} + 7.56, \quad (5)$$

where p^0 is 101 325 Pa. When the total pressure ($p_{tot}/p^0 = -35520(T/K)^{-1} + 8.26$ [17]) is corrected with the above equations, Ackermann and Rauh obtained for the partial pressure of ThO_2:

$$\log(p_{ThO_2}/p^0) = -35070(T/K)^{-1} + 7.96 \quad (6)$$

When this equation is analyzed by the third-law method, the value $\Delta_{sub}H^0(298.15\ K) = 770$ kJ mol^{-1} is obtained. The agreement with the second-law value is poor and, moreover, a clear temperature trend exists in the third-law analysis. The third-law analyses of the other vapour pressure studies are summarized in Table 2. Except for the studies by Hoch and Johnston [15] and Alexander et al. [18], the studies are in reasonable agreement and the third-law enthalpies of sublimation range from 759 to 773 kJ mol^{-1}. Taking into account the above noted uncertainties and the difficulties that occur during experiments at such high temperatures, we recommend for the enthalpy of sublimation of ThO_2 the value

$$\Delta_{sub}H^0 = (770 \pm 10)\ \text{kJ mol}^{-1}. \quad (7)$$

The thermodynamic data for ThO_2(g) that have been used in the third-law analysis are calculated from the following molecular parameters which are listed in Table 3 and are based on the following studies. The bent structure of the ThO_2 molecule has been derived from matrix-isolation by Gabelnick et al. [22] and Linevsky [23] and from molecular beam deflection studies by Kaufman et al. [24]. The bond angles derived from the matrix-isolation data are 122.5° and 106°, respectively, the former value being considered the most accurate due to the higher resolution of the spectral data. The stretching frequencies from the two matrix-isolation studies are in excellent agreement, the bending frequency has not been observed and has been estimated from analogies with other gaseous metal dioxides.

2.5. Thermal conductivity of ThO_2

The thermal conductivity of ThO_2 up to 1800 K is reasonably well established. Most of the data were derived from thermal diffusivity measurements. The studies listed in Table 4 are in reasonable agreement, as shown in Fig. 2. Not shown in Fig. 2 are the data by Wechsler and Glaser [25] which are exceptionally low, due to the high porosity of the sample. Data as measured by Pears [26] are also not shown, since these thermal conductivity data are also very low, which is probably due to a poor sample quality. According to Touloukian et al. [27] the sample of Pears has a 'poorly bonded' structure and was found broken on post inspection. Data of Rodriguez et al. [28], McEwan

Table 3
The molecular parameters for ThO_2(g)

Parameter	Value
Symmetry group	C_{2v}
Symmetry number σ	2
r(Th–O) distance	182 ± 6 pm
∠(O–Th–O) angle	122.5°
Vibrational frequencies (degeneracy)	787, 220(2), 735 cm^{-1}
Moment of inertia $I_A I_B I_C$	8.282 10^{-115} g^3 cm^6
Electronic levels	ground state only, $g_0 = 1$

Table 4
Thermal conductivity measurements for ThO_2

T (K)	Density	Authors	Year
373, 1473	corr. to 100%	Warde [32]	?
304–379	95.4%	Koenig [43]	1953
373–1273	unknown	Kingery et al. [35]	1954
538–1593	80.4%	Adams [94]	1954
527–824	93.3%	ARF [39]	1957
300–1673	corr. to 100%	Bradshaw and Mathews [95]	1958
1273	corr. to 100%	Whittemore [33]	1959
400–1366	91.6%	DeBosky [41]	1962
1331–1821	96.5%	Pears [26]	1963
1219–2009	unknown	Wechsler and Glaser [25]	1963
373–1473	unknown	Peterson [31]	1966
393	various	Belle et al. [30]	1967
303, 393	95.0%	Moore et al. [96]	1967
573–2173	various	Springer et al. [9]	1967
200–1400	92.7%	McElroy et al. [36]	1968
333	95.0%	McEwan and Stoute [29]	1969
300–1173	94.0%	Murabayashi [69,42]	1969, 1970
1900–2600	91.6%	Faucher et al. [34]	1970
400–2550	97.0%	Weilbacher [40]	1972
773, 1773	unknown	Rodriguez et al. [28]	1981
573–1573	92.0%	Srirama Murti and Mathews [70]	1991

and Stoute [29], Belle et al. [30], Peterson et al. [31], Warde [32] and of Whittemore [33] (see Ref. [93]) were discarded since insufficient information is available. Data of Faucher et al. [34] were rejected since the temperature range of measurement is very high and the data shows large scatter. Data of Kingery et al. [35] were rejected since problems occurred with the density and the stoichiometry of their samples. The data of McElroy et al. [36] consists of two fits (200–400 K and 400–1400 K). Only the high temperature curve has been used in the present analysis, since this is the temperature range of interest in the present study.

The data shown in Fig. 2 were corrected, in the present investigation, to 95% theoretical density using Eq. (8):

$$f = (1 - P)^{1.5}, \tag{8}$$

where $P(0 < P < 1)$ is the porosity and f is the fraction of the thermal conductivity $(0 < f < 1)$. This equation describes the influence of randomly ordered, spherical porosity on the thermal conductivity [37].

In order to assess the data all measurements were fit to Eq. (9), after correction of the measurements to 95% theoretical density:

$$\lambda = \frac{1}{A + B(T/\mathrm{K})}, \tag{9}$$

where λ ($\mathrm{W\,m^{-1}\,K^{-1}}$) is the thermal conductivity and A ($\mathrm{m\,K\,W^{-1}}$) and B ($\mathrm{m\,W^{-1}}$) are parameters. At the operational temperatures of nuclear fuel (300–1800 K) this equation holds both for ThO_2 and UO_2. The parameter A represents the influence of phonon scattering by lattice imperfections. The parameter B describes the influence of phonon–phonon scattering. The influence of substitutions on the thermal conductivity is described by an increase of the parameter A, while parameter B remains nearly constant on substitution. The parameter A depends on the difference in mass and radius between the substituted atom and the host atom [38]. The A and B parameters obtained from the ThO_2 data shown in Fig. 2 are presented in Fig. 3.

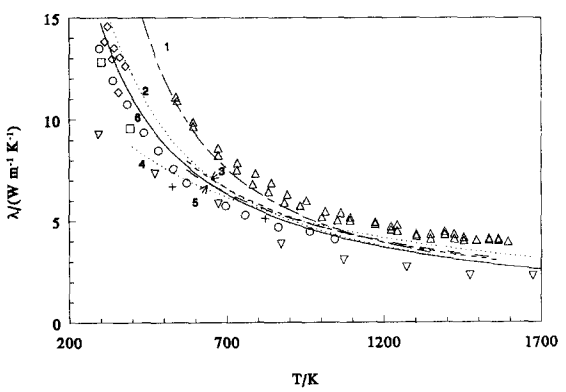

Fig. 2. The thermal conductivity of ThO_2, the data have been corrected to 95% theoretical density using Eq. (8); +, ARF; △, Adams; ◇, Koenig; ○, Murabayashi, □, Moore et al.; ▽, Bradshaw and Mathews; curve 1, DeBoskey; curve 2, McElroy et al.; curve 3, Springer et al.; curve 4, Weilbacher; curve 5, Srirama Murti and Mathews; curve 6, Recommended curve. The references are given in Table 4.

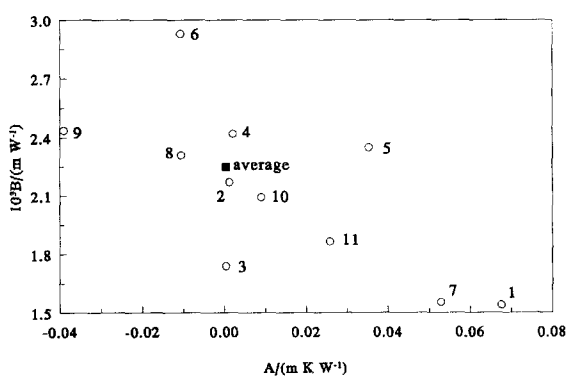

Fig. 3. The A and B parameters in Eq. (8) obtained for the ThO_2 data shown in Fig. 2 for a porosity of 5%. 1 ARF, 2 Koenig, 3 Adams, 4 Murabayashi, 5 Bradshaw an Mathews, 6 Moore et al., 7 Weilbacher, 8 McElroy, 9 DeBoskey, 10 Springer et al., 11 Srirama and Mathews. The square represents the average value that is obtained from the data of Murabayashi, McElroy et al., Koenig and Springer et al.. The references are given in Table 4.

We have chosen to assess the data by investigating the A and B-parameters rather than by averaging the thermal conductivity values of all the data sets. Assessing the A and B-parameters has the advantage that data sets that were determined in different temperature ranges can easily be compared and that data sets with extremely large or small A and B-parameters can be rejected. The large A parameters of ARF [39] and Weilbacher [40] suggest that their samples are impure, while the negative A parameter of DeBoskey [41] is in contradiction with the model. Only a small variation exists between the A and B parameters of Murabayashi [42], McElroy et al. [36], Koenig [43] and Springer et al. [9]. These data are more or less in the center of the other data sets. The A and B parameters were averaged, which yielded $A = 4.20 \times 10^{-4}$ m K W^{-1} and $B = 2.25 \times 10^{-4}$ m W^{-1}. These values can be used as the recommended values for 95% dense ThO_2 in the temperature range between 300 K and 1800 K.

2.6. Linear thermal expansion of ThO_2

ThO_2 has a face-centered cubic crystal structure (space group $Fm\bar{3}m$) from room temperature up to the melting point. At room temperature the lattice parameter is 0.55970(3) nm [44].

The linear thermal expansion of ThO_2, which is isotropic for the fluorite-type structure, is well established: Touloukian et al. [45] list more than 30 different measurements which are in excellent agreement and we therefore adopt the equation recommended by Touloukian (150 to 2000 K):

$$\Delta L/L_0 = -0.179 + 5.097 \times 10^{-4}(T/\mathrm{K}) + 3.732 \times 10^{-7}(T/\mathrm{K})^2 - 7.594 \times 10^{-11}(T/\mathrm{K})^3, \quad (10)$$

where the linear thermal expansion is $\Delta L/L_0$ (in %). ΔL is zero at 293 K.

3. $Th_{1-y}U_yO_2$

3.1. Phase diagram of UO_2–ThO_2

Solid UO_2 and ThO_2 form a continuous series of solid solutions [46]. Lattice parameter measurements of UO_2–ThO_2 solutions show that, within experimental accuracy, Vegard's law is obeyed. This indicates that this solution can be regarded as an ideal solid mixture. Slowinski and Elliott [47] as well as Lambertson et al. [46] showed that ThO_2 and UO_2 form an ideal solid solution in the whole composition range. The lattice parameter of this cubic (fluorite-type) solution was found to decrease linearly from 100% ThO_2 to 100% UO_2 in both studies, as shown in Fig. 4. The absolute values from both studies differ somewhat but the results of Lambertson et al. were confirmed by Kanno et al. [48]. The results by Trzebiatowski and Selwood [49] and Christensen [50] deviate from the linear relation suggesting some departure from ideality.

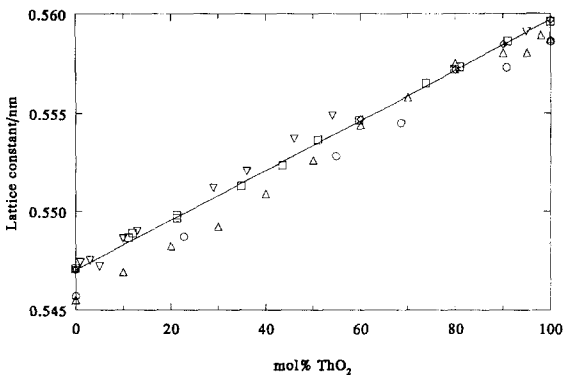

Fig. 4. The lattice parameter of the $Th_{1-y}U_yO_2$ solid solution; ○, Slowinski and Elliott; △, Trzebiatowski and Selwood; □, Lambertson et al.; ◇, Kanno et al.; ▽, Christensen, The line represents a linear relation between the recommended value for ThO_2 [44] and a recommended value for UO_2 [98].

The phase diagram of UO_2–ThO_2 has not yet been satisfactorily established. This is partly due to experimental problems with the measurements of the solidus and liquidus lines. The high melting temperature is difficult to determine accurately and preferential evaporization of UO_2 may change the actual composition of the mixture.

Measurements of the phase diagram of UO_2–ThO_2 were performed by Christensen [50] using the tungsten filament technique, by Lambertson et al. [46] using a quench technique and by Latta et al. [51] using the thermal arrest method.

The solidus and liquidus points are plotted in Fig. 5. Both the measurements of Christensen and Latta et al.

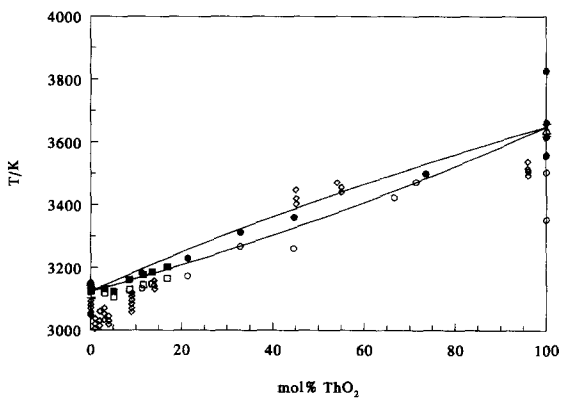

Fig. 5. Phase diagram of UO_2–ThO_2. The solid lines refer to calculated lines. The filled symbols refer to solidus points, the open symbols refer to liquidus points. □ Latta et al. [51]; ○ Lambertson et al. [46]; ◇ Christensen [50]; △ melting point of ThO_2 [12]; ▽ melting point of UO_2 [97].

Table 5
Melting points and enthalpies of fusion of UO_2, ThO_2 PuO_2 used for the calculation of the ideal phase diagrams. The enthalpy of fusion of ThO_2 is taken from Ref. [97]

Compound	$\Delta_{fus}H^0$ (kJ mol^{-1})	T_{fus} (K)	Ref.
UO_2	78	3123 ± 20	Glushko [97]
ThO_2	90	3651 ± 17	see Table 1
PuO_2	67 ± 15	2663 ± 40	Cordfunke and Konings [98]

show a shallow minimum at 2 and 5 mol% ThO_2, respectively. There is still some uncertainty in the melting point of UO_2, which has a strong dependence on the stoichiometry.

A comparison with the phase diagram of an ideal mixture was made. The solidus and liquidus for an ideal mixture were calculated using values tabulated in Table 5. Furthermore, it was assumed that the heat capacity of the liquid and solid pure components are equal. The result is shown in Fig. 5. Clearly the UO_2–ThO_2 phase diagram still shows large uncertainties. These uncertainties may partly be due to differences in gas atmosphere, i.e., helium gas versus oxygen gas.

3.2. Heat capacity

The heat capacity of the $Th_{1-y}U_yO_2$ solid solution has been measured indirectly by enthalpy drop calorimetry by Springer et al. [9] from 573 to 2173 K for samples containing 10.3 and 20.4 wt% UO_2 and by Fischer et al. [52] from 2300 to 3400 K for the compositions $Th_{0.70}U_{0.30}O_2$, $Th_{0.85}U_{0.15}O_2$ and $Th_{0.92}U_{0.08}O_2$. The only composition for which the two data sets can be compared

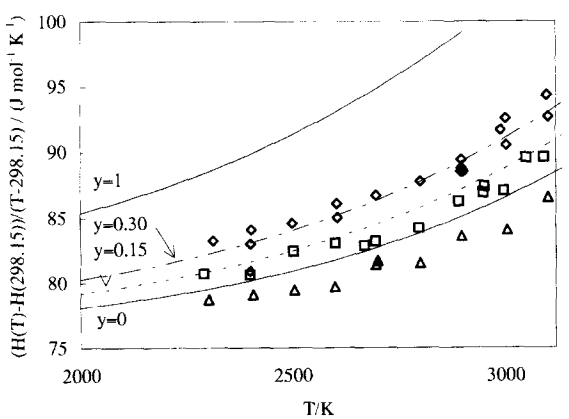

Fig. 6. The reduced enthalpy increment of $Th_{1-y}U_yO_2$ (Fischer et al.) up to the melting temperature of UO_2 for △, $y = 0.08$; □, $y = 0.15$; ◇, $y = 0.30$. The drawn lines are the molar averages of the reduced enthalpy increment functions of ThO_2 and UO_2 for different values of y. The enthalpy increment function of UO_2 is taken from Ref. [98].

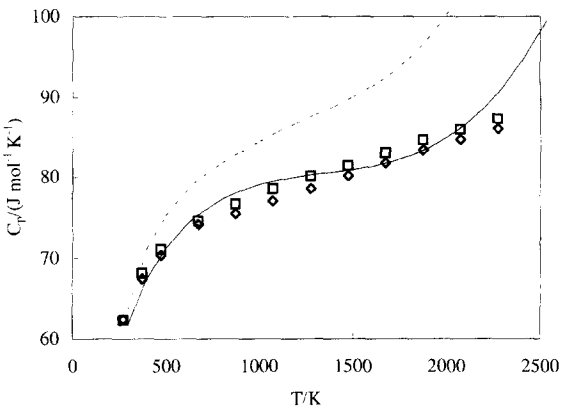

Fig. 7. Heat capacity of $Th_{1-y}U_yO_2$ (Springer et al.) for □, 20.4 wt% UO_2; ◇, 10.3 wt% UO_2; Solid line, heat capacity of ThO_2; Dashed line, heat capacity of UO_2.

is about $Th_{0.9}U_{0.1}O_2$. For this composition the results from both studies are in good agreement. However, the data by Springer et al. are somewhat too high at lower temperatures, as are their data for pure ThO_2.

The results by Fischer show that the enthalpies of the compositions $Th_{0.70}U_{0.30}O_2$, $Th_{0.85}U_{0.15}O_2$ are almost identical with the mole averages of the pure compounds (Fig. 6), whereas the enthalpy of the composition $Th_{0.92}U_{0.08}O_2$ is somewhat lower than that of pure ThO_2. The heat capacities of Springer et al. (Fig. 7) show a different trend than the data of pure ThO_2.

3.3. Vapour pressure

The partial pressure of UO_2 over $Th_{1-y}U_yO_2$ has been measured by Alexander et al. [18] for two different compositions (7.97 wt% and 20.3 wt% UO_2) using the transpiration technique, but in view of his deviating results for pure

Table 6
Oxygen potential measurements of $Th_{1-y}U_yO_{2+x}$

y-range	T (K)	Method [a]	Authors	Year
0.03–0.244	1000–1200	TGA/V	Anderson et al. [99]	1954
0.0053–0.0597	1123	PM	Roberts et al. [100]	1958
0.29–1	1250	EMF	Aronson and Clayton [101]	1960
0.048–0.295	1250	EMF	Tanaka et al. [102]	1972
0.05–1	1273–1473	TGA	Ugajin et al. [103–105]	1982
0.2–1	1282–1373	TGA	Matsui and Naito [106]	1985

[a] EMF = electromotive force measurements; TGA = thermogravimetric analysis; V = gas volumetric method; PM = pressure measurement.

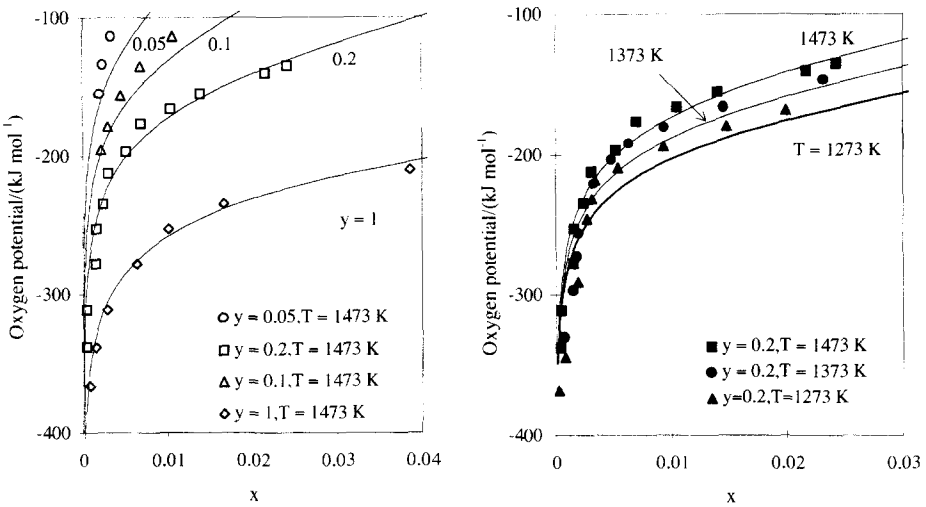

Fig. 8. Temperature- and y-dependence of the oxygen potentials of $Th_{1-y}U_yO_{2+x}$. Experimental points: Ugajin et al. [103–105]. Solid lines are calculated using Eq. (13) and the parameters of Table 7.

ThO_2 the results should be used with caution. The activity of ThO_2 was found to be nearly unity and an ideal behaviour was observed.

3.4. Oxygen potential

The oxygen potential, the partial molar Gibbs energy of oxygen per mole of O_2 in a condensed phase, is defined as

$$\Delta\overline{G_{O_2}} = RT \ln p_{O_2}. \tag{11}$$

The oxygen potential of $Th_{1-y}U_yO_2$ has been measured by various authors for a wide range of compositions, as summarized in Table 6. The oxygen potential of $Th_{1-y}U_yO_{2+x}$ increases with increasing temperature and with increasing x, similar to the oxygen potential of UO_{2+x} [53]. The oxygen potential of $Th_{1-y}U_yO_{2+x}$ increases with decreasing amount of uranium y as can be seen in Fig. 8. Oxygen potential data of $Th_{1-y}U_yO_{2+x}$ were stored in a database and were analyzed using a defect model approach and a thermochemical model [54].

Several defect models for UO_{2+x} [55–58] and for $Pu_{1-y}U_yO_{2+x}$ [59,60] were published but no defect models for $Th_{1-y}U_yO_{2+x}$ were found in literature. Park and Olander developed a defect model for UO_{2+x} [58], for Gd and Eu doped urania [61], and Wang et al. [62] published a model for urania–neodymia mixed oxides. All these defect models consider the formation of so-called Willis clusters. Willis [63] studied the defect structure of $UO_{2.13}$ using neutron diffraction and found that interstitial oxygen forms a cluster with vacancies on regular oxygen sites. Two different interstitial oxygen positions were found, O_i^a and O_i^b. Willis proposed that clusters $V_O^{\cdot\cdot}:O_i^a:O_i^b$ with the ratios 2:1:2 and 2:2:2 may be present in urania. More recently, Murray and Willis [64] performed new neutron diffraction measurements on UO_{2+x} ($x \approx 0.11$–0.13) and found evidence for 2:2:2 clusters and cuboctahedral clusters.

Lindemer and Besmann [53] described the oxygen potential of UO_{2+x} by considering this oxide as a binary mixture of stoichiometric UO_2 and U_aO_b. This model was extended for $Th_{1-y}U_yO_{2+x}$ [54] and it was assumed that the oxidation state of thorium does not change with the oxygen pressure, and as a consequence, thorium oxide does not appear in the chemical equilibrium describing the oxygen potential:

$$\frac{2a}{b-2a}UO_2 + O_2 = \frac{2}{b-2a}U_aO_b. \tag{12}$$

In this model $Th_{1-y}U_yO_{2+x}$ is considered as ideal ternary solution of UO_2, ThO_2 and U_aO_b and the mole fraction of these components is calculated from the mass balance for

Table 7
Fit parameters of for the description of the oxygen potential of $Th_{1-y}U_yO_{2+x}$, Eq. (13)

Oxygen potential range	a	b	$\Delta_r H^0$ (kJ mol^{-1})	$\Delta_r S^0$ (J K^{-1} mol^{-1})
< -100 kJ mol^{-1}	1.336	3.323	−393.4	−198.01
> -100 kJ mol^{-1}	1.974	5.219	−176.0	−81.5

Table 8
Thermal conductivity measurements for $Th_{1-y}U_yO_2$

y-values (%)	T (K)	Authors	Year
0, 10, 26, 31, 100	373–1070	Kingery [107]	1959
0, 8, 10	570–1100	DeBoskey [41]	1962
5, 9, 14, 19	power to melt	Rao [108,109]	1963
10, 100	1073–2073	Harbinson and Walker [110]	1966
0, 10, 20, 30, 50, 90, 100	393	Belle et al. [30]	1967
4.7, 6.1, 6.3	293–423	Moore et al. [96]	1967
0, 10, 20	573–2173	Springer et al. [9]	1967
3, 5, 7, 10, 13, 20, 25, 30, 100	573–2173	Springer and Lagedrost [10]	1968
0, 1.3	333	MacEwan and Stoute [29]	1969
0, 1, 5, 10	293–773	Murabayashi et al. [69]	1969
0, 1, 3, 5, 10	298–1073	Murabayashi [42]	1970
6, 10	923–2973	Ferro et al. [111]	1972
0, 20, 100	773, 1773	Rodriguez and Sundaram [28]	1981
5	370–1673	KWU [112]	1988
2	800–2100	Basak et al. [83]	1989

U, Th and O. In this model the oxygen potential of $Th_{1-y}U_yO_{2+x}$ is given by

$$RT \ln p_{O_2} = \frac{2}{b-2a} RT \ln \frac{[U_aO_b]}{[UO_2]^a} + \Delta_r H^0 - T\Delta_r S^0, \quad (13)$$

where $\Delta_r H^0$ and $\Delta_r S^0$ are the enthalpy and entropy of the reaction described in Eq. (12), and the activity $[U_aO_b]$ and $[UO_2]$ can be expressed in terms of x, y, a and b. Eq. (13) was fitted to the oxygen potential data listed in Table 6. The oxygen potential was divided in two ranges, demarcated by -100 kJ mol^{-1}. The results of the fits are shown in Table 7. The average relative error is 6% for oxygen potentials lower than -100 kJ mol^{-1} and 22% in the other range.

3.5. Thermal conductivity of $Th_{1-y}U_yO_2$

In Table 8 an overview of the thermal conductivity measurements on $Th_{1-y}U_yO_2$ is given. An assessment of thermal conductivity data of both irradiated and unirradiated ThO_2 and $Th_{1-y}U_yO_2$ solid solutions has been made by Berman et al. [65]. They analyzed data of Springer et al. [9,10], Jacobs [66,67], Matolich and Storhok [68] and Belle et al. [30]. Berman et al. suggested complex behaviour of the parameters A and B of Eq. (9) on variation of the uranium content which is inconsistent with theory and data on other ThO_2 or UO_2 compounds containing substitutions. For these reasons the assessment of Berman et al. has been rejected.

Most authors observed that the thermal conductivity decreases with UO_2 content. In this assessment only those data sets have been used that

- contain pure ThO_2,
- show a systematic decrease of the thermal conductivity on increasing UO_2 content (for UO_2 concentrations up to 20%),
- contain the temperature dependence of the thermal conductivity.

These criteria left only the data of Murabayashi [69,42] and Springer et al. [9], see Fig. 9. Of the two data sets of Murabayashi, that show good agreement, only the most recent set [42] has been used.

For both data sets shown in Fig. 9 the parameters A and B have been determined for various UO_2 contents, see Fig. 10. The data of Murabayashi were corrected to 95% theoretical density using Eq. (8) before determining these parameters. The variation of the parameters A and B on UO_2 substitution is very different for both data sets. In order to analyze these parameter sets, the behaviour of these parameters in other ThO_2 and UO_2 compounds containing substitutions is discussed in the next paragraph.

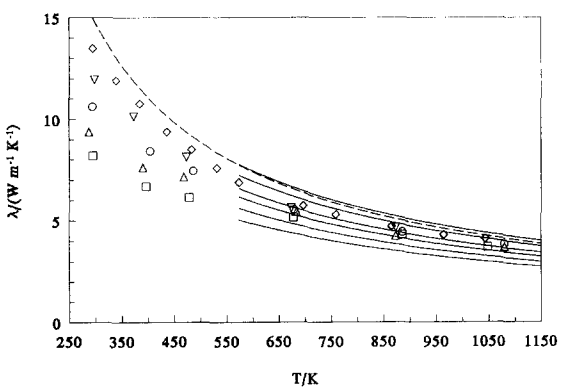

Fig. 9. The thermal conductivity of $Th_{1-y}U_yO_2$; the data have been corrected to 95% density using Eq. (8). The experimental data are from Murabayashi [42], ◇, $y = 0$; ▽, 0.01; ○, 0.03; △, 0.05; □, 0.10. The six solid lines are obtained from Springer et al. [9] for $y = 0.0$, 0.01, 0.03, 0.05, 0.10, 0.20 (higher concentration corresponds to lower conductivity). The broken line represents the recommended value for ThO_2.

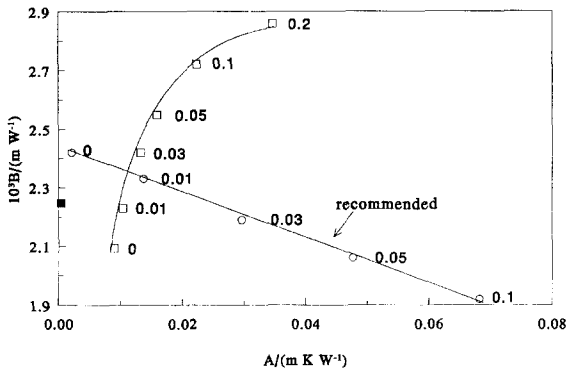

Fig. 10. The A and B parameters in Eq. (9) for a porosity of 5% obtained from the $Th_{1-y}U_yO_2$ data shown in Fig. 9. The circles represent the parameters obtained from the data of Murabayashi [42] for $y = 0.0, 0.01, 0.03, 0.05, 0.10$. The squares represent the parameters obtained from the equation of Springer and Lagedrost [10] for $y = 0.0, 0.01, 0.03, 0.05, 0.10, 0.20$. The black square represents the recommended A and B value for ThO_2.

Srimara Murti and Mathews performed thermal conductivity measurements on ThO_2 containing between 0 mol% and 30 mol% of $LaO_{1.5}$ [70] and $EuO_{1.5}$ [71]. They observed a strong, nearly linear, increase of the A-parameter on these substitutions and found a relatively small increase of the B-parameter for $LaO_{1.5}$ and for $EuO_{1.5}$ substitutions up to 20 mol%. For 25 and 30 mol% the B-parameter starts to decrease. Lucuta et al. [72] observed in UO_2 containing simulated fission products a linear increase of the A-parameter on substitution, while the B-parameter shows a very small decrease on substitution. Fukushima et al. [73] measured the thermal conductivity of UO_2, PuO_2 and their mixed oxides containing rare earths. In all these compounds the A-parameter shows a strong increase on substitution, while the B-parameter shows a small decrease on substitution, except for $(U, Y)O_{2-x}$ solid solutions where the B-parameter slightly increases on substitution [74].

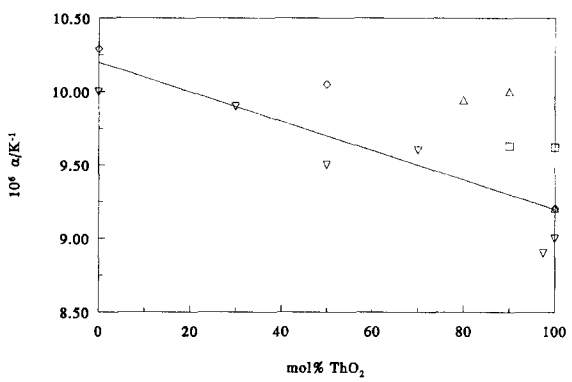

Fig. 11. The relation between the uranium content y in $Th_{1-y}U_yO_2$ and the average linear thermal expansion coefficient between 293 K and 1173 K for the data sets of: □, Kempter and Elliot [75]; ▽, Lynch and Beals [76]; △, Springer et al. [9] and ◇, Turner and Smith [77]. The line represents a linear relation between the average linear thermal expansion coefficient of ThO_2 [45] and UO_2 [80].

Since good agreement exists between the variation of the A and B-parameter on substitution as determined by Murabayashi and the variation of A and B of comparable compounds as well as that predicted by theory, these parameters are used to obtain a recommended thermal conductivity for $Th_{1-y}U_yO_2$. In order to make this recommendation the difference between the thermal conductivity of ThO_2 as measured by Murabayashi and the recommended value for ThO_2 as discussed in this paper is corrected for. This is done by increasing the thermal conductivity values of $Th_{1-y}U_yO_2$ of Murabayashi with the difference between the Murabayashi A and B value of ThO_2 and the recommended A and B value of ThO_2.

The uranium concentration dependence of the thus obtained A and B parameters was fitted to obtain an equation that is valid for an uranium concentration up to 10% and a theoretical density of 95%:

$$A = 4.195 \times 10^{-4} + 1.112\,y - 4.499\,y^2$$
$$B = 2.248 \times 10^{-4} - 9.170 \times 10^{-4}\,y + 4.164 \times 10^{-3}\,y^2 \quad (14)$$

These parameters, combined with Eq. (9), yield the recommended thermal conductivity of $Th_{1-y}U_yO_2$ in the temperature range between 300 K and 1173 K, for uranium concentrations up to 10%.

3.6. Linear thermal expansion of $Th_{1-y}U_yO_2$

In order to assess the influence of uranium substitution on the linear thermal expansion we have determined the average linear thermal expansion coefficient

$$\bar{\alpha} = \frac{1}{L_0}\frac{\Delta L}{\Delta T} \quad (15)$$

between 293 K and 1173 K for the data sets of Kempter and Elliot [75], Lynch and Beals [76], Springer et al. [9], Turner and Smith [77] and that of Momin et al. [78], see Fig. 11. All these authors, except Momin et al., find that the average linear thermal expansion coefficients of $Th_{1-y}U_yO_2$ $(0 < y < 1)$ compounds fall between those of ThO_2 and UO_2, within experimental accuracy. Momin et al. [78], who made the most recent expansion study, using X-ray diffraction, found that the linear thermal expansion coefficient of $Th_{0.8}U_{0.2}O_2$ is much smaller than that of both ThO_2 and UO_2. Since no explanation was given for this unexpected result and no comparison was made with earlier studies the measurements of Momin et al. were discarded. Powers and Shapiro [79] mention an average linear thermal expansion coefficient of 9×10^{-6} K^{-1} for $Th_{0.936}U_{0.064}O_2$ (up to 1073 K), 8×10^{-6} K^{-1} for $Th_{0.8}U_{0.2}O_2$ (up to 1073 K), 9×10^{-6} K^{-1} for UO_2.

They observed that substitution of 1% of Y_2O_3 has a strong influence on the linear thermal expansion. Since no measurement on ThO_2 was performed and the data have a low accuracy (only one digit), these data were not included in Fig. 11. Rodriguez and Sundaram [28] report an average linear thermal expansion coefficient of 10.0×10^{-6} K^{-1} for UO_2 (273–1273 K), 9.67×10^{-6} K^{-1} for ThO_2 (293–2273 K) and 12.5×10^{-6} K^{-1} for $Th_{0.8}U_{0.2}O_2$ (1100–2400 K). Since the temperature ranges for which these averages where determined differ and no further information was given in this paper, these data are not taken into account.

In Section 3.1 it has been discussed that ThO_2 and UO_2 form an ideal solid solution in the whole composition range. It was discussed that, at room temperature, the lattice parameter decreases linearly from 100% ThO_2 to 100% UO_2. Considering that the vapour pressure measurements [18] indicate an ideal solution behaviour at high temperatures, we assume that this linear decrease in the lattice parameter also exists at high temperature. This linear decrease can only exist when the linear thermal expansion of $Th_{1-y}U_yO_2$ $(0 < y < 1)$ equals the linearly interpolated value of that of ThO_2 and that of UO_2. This is in reasonable agreement with the experimental data shown in Fig. 11. The recommended value of the linear thermal expansion of $Th_{1-y}U_yO_2$ $(0 < y < 1)$ in % is obtained by linear interpolation of the values of ThO_2 (Eq. (10), [45]) and UO_2 [80]:

$$\begin{aligned}\Delta L/L_0 = &-0.179 - y0.087 \\ &+ (5.09710^{-4} + y4.705 \times 10^{-4})(T/\mathrm{K}) \\ &+ (3.73210^{-7} - y4.002 \times 10^{-7})(T/\mathrm{K})^2 \\ &- (7.594 \times 10^{-11} - y11.98 \times 10^{-11})(T/\mathrm{K})^3 \end{aligned} \quad (16)$$

for $273 \leq T/\mathrm{K} \leq 923$ and

$$\begin{aligned}\Delta L/L_0 = &-0.179 - y0.149 \\ &+ (5.097 \times 10^{-4} + y6.693 \times 10^{-4})(T/\mathrm{K}) \\ &+ (3.732 \times 10^{-7} - y6.161 \times 10^{-7})(T/\mathrm{K})^2 \\ &- (7.594 \times 10^{-11} - y19.784 \times 10^{-11})(T/\mathrm{K})^3 \end{aligned} \quad (17)$$

for $923 \leq (T/\mathrm{K}) \leq 2000$.

4. $Th_{1-y}Pu_yO_2$

Freshley and Mattys [81] have shown that ThO_2 and PuO_2 form an ideal solid solution in the whole composition range, like ThO_2 and UO_2. The lattice parameter of this cubic (fluorite-type) solution was found to decrease regularly from 0.5586 nm for ThO_2 to 0.5396 nm for PuO_2.

Few data of the phase diagram of this system were found. The melting point of the ThO_2–PuO_2 binary system

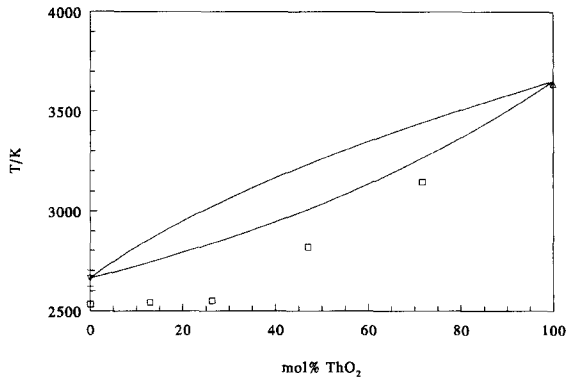

Fig. 12. Phase diagram of PuO_2–ThO_2. The solid lines refer to the ideal mixing behaviour. □ melting points of $Th_{1-y}Pu_yO_2$ [82]; △ melting point of ThO_2 [12]; ▽ melting point of PuO_2 [98].

was measured in helium on a tungsten filament [82]. The results are shown in Fig. 12 together with the ideal phase diagram that was calculated using the parameters of Table 5. The melting point of a PuO_2 sample, whose purity was not specified, tabulated in [82] is 2533 K, which is 130 K lower than the assessed value of Table 5. Due to the limited amount of experimental data a more accurate assessment of the phase diagram of the ThO_2–PuO_2 system is not yet possible.

4.1. Thermal conductivity of $Th_{1-y}Pu_yO_2$

Very few thermal conductivity measurements were made on $Th_{1-y}Pu_yO_2$ [83–85]. Basak et al. [83] measured the thermal conductivity of $Th_{0.96}Pu_{0.04}O_2$ using the laser flash technique. Jeffs [84,85] determined the integrated thermal conductivity of $Th_{1-y}Pu_yO_2$ containing 1.10, 1.75 and 2.72 wt% PuO_2 by irradiation of three fuel elements with a central thermocouple. Jeffs observed that the integrated thermal conductivity of these compounds is larger than that of UO_2. Since both authors did not measure ThO_2 and they used only very low Pu concentrations, their data cannot be used to assess the thermal conductivity of $Th_{1-y}Pu_yO_2$. Data for the heat capacity, vapour pressure, linear thermal expansion and oxygen potential of this solid solution are not available.

5. Conclusion

The thermal properties of ThO_2 and $Th_{1-y}U_yO_2$ were assessed and the very limited amount of data on $Th_{1-y}Pu_yO_2$ was surveyed. For ThO_2 and $Th_{1-y}U_yO_2$ the phase diagram, heat capacity, vapour pressure, oxygen potential, thermal conductivity and linear thermal expansion were discussed. The information on these properties is sufficient to recommend values for the low uranium concentration range ($y < 0.2$) that is of interest to the application of thoria based fuel in LWRs. In this concentration

range uranium substitution decreases the lattice parameter, melting point, oxygen potential, thermal conductivity, while it increases the density and the linear thermal expansion. The most drastic change, and the most important change from nuclear fuel point of view, is the decrease of the thermal conductivity on increasing uranium concentration ($y < 0.2$). In the uranium concentration range $y > 0.2$ less data are available. Also for this concentration range the lattice parameter, melting point and oxygen potential decrease and the linear thermal expansion increases on uranium substitution. In the concentration range ($y > 0.2$) no assessment could be made of the vapour pressure, the thermal conductivity and the heat capacity.

The amount of data on the thermal properties of $Th_{1-y}Pu_yO_2$ is very limited. The reason for this is twofold: measurements on plutonium containing compounds require extensive safety precautions and are thus expensive moreover, the plutonium concentration in $Th_{1-y}Pu_yO_2$ that will be used as a nuclear fuel in LWRs is probably smaller than 10%, which strongly limits the concentration range of interest. For fast reactors the plutonium concentration of interest can be as high as 40%.

The magnitude of the difference between the thermal properties of $Th_{1-y}Pu_yO_2$ and ThO_2 can be estimated from theory and from the difference between the properties of ThO_2 and $Th_{1-y}U_yO_2$. From this it is expected that at low Pu concentrations the thermal properties of $Th_{1-y}Pu_yO_2$ are rather similar to those of ThO_2. Due to this expected similarity, technological efforts should be mainly directed to the behaviour of $Th_{1-y}Pu_yO_2$ fuel during irradiation [86,87], since irradiation experiments yield information on the complex interplay of thermal and mechanical properties.

References

[1] J.D. Cox, D.D. Wagman, V.A. Medvedev, CODATA Key Values for Thermodynamics (Hemisphere, New York, 1989).

[2] E.J. Huber Jr., C.E. Holley Jr., E.H. Meierkord, J. Am. Chem. Soc. 74 (1952) 3406.

[3] W.A. Roth, G. Becker, Z. Phys. Chem. A159 (1932) 1.

[4] D.W. Osborne, E.F. Westrum Jr., J. Chem. Phys. 21 (1953) 1884.

[5] F.M. Jaeger, W.A. Veenstra, Proc. R. Acad. Sci. (Amsterdam) 37 (1927) 327.

[6] J.C. Southard, J. Am. Chem. Soc. 63 (1941) 3142.

[7] M. Hoch, H.L. Johnston, J. Phys. Chem. 65 (1961) 1184.

[8] A.C. Victor, T.B. Douglas, J. Res. Nat. Bur. Stand. A65 (1961) 105.

[9] J.R. Springer, E.A. Eldridge, M.U. Goodyear, T.R. Wright, J.F. Langedrost, Battelle Memorial Institute Report BMI-X-10210, 1967.

[10] J.R. Springer, J.F. Langedrost, Battelle Memorial Institute Report BMI-X-10231, 1968.

[11] D.F. Fischer, J.K. Fink, L. Leibowitz, J. Nucl. Mater. 102 (1981) 220.

[12] C. Ronchi, J.P. Hiernaut, J. Alloys Comp. 240 (1996) 179.

[13] J.K. Fink, M.G. Chasanov, L. Leibowitz, Argonne National Laboratory Report, ANL-CEN-RSD-77-1, 1977.

[14] E. Shapiro, J. Am. Chem. Soc. 74 (1952) 5233.

[15] M. Hoch, H.L. Johnston, J. Am. Chem. Soc. 76 (1954) 4833.

[16] A.J. Darnell, W.A. McCollum, Atomics International Report NAA-SR-6498, 1961.

[17] R.J. Ackermann, E.G. Rauh, M.C. Cannon, J. Phys. Chem. 67 (1963) 762.

[18] C.A. Alexander, J.S. Ogden, G.W. Cunningham, Battelle Memorial Institute Report BMI-1789, 1967.

[19] J. Cears, F.G. Casteels, M.J. Brabers, High. Temp.-High Press. 12 (1980) 411.

[20] E.J. Ackermann, E.G. Rauh, High Temp. Sci. 5 (1973) 463.

[21] A.N. Belov, G.A. Semenov, Z. Fiz. Khim. 54 (1980) 1537.

[22] S.D. Gabelnick, G.T. Reedy, M.G. Chasanov, J. Chem. Phys. 60 (1974) 1167.

[23] M.J. Linevsky, Report AD-611856, 1965.

[24] M. Kaufman, J. Muenter, W. Klemperer, J. Chem. Phys. 47 (1967) 3365.

[25] A.E. Wechsler, P.E. Glaser, Report ASD-TR-63-574, 1963, cited in Ref. [27].

[26] C.D. Pears, Report ASD-TR-62-765, 1957, cited in Ref. [27].

[27] Y.S. Touloukian, R.W. Powell, C.Y. Ho, P.G. Klemens, Thermal Conductivity. Nonmetallic Solids (IFI/Plenum, New York, 1970).

[28] P. Rodriguez, C.V. Sundaram, J. Nucl. Mater. 100 (1981) 227.

[29] J.R. MacEwan, R.L. Stoute, J. Am. Ceram. Soc. 52 (1969) 160.

[30] J. Belle, R.M. Berman, W.F. Bourgeois, I. Cohen, R.C. Daniel, Westinghouse Report WAPD-TM-586.

[31] S. Peterson, R.E. Adams, D.A. Douglas, International Atomic Energy Agency Report STI/DOC/10/52, Vienna, 1966, cited in: L.R. Weissert, G. Schileo, Fabrication of Thorium Fuel Elements (American Nuclear Society, 1968).

[32] J.M. Warde, Refractories Institute Pittsburgh, Technical Bulletin No. 94, cited in Ref. [93].

[33] O.J. Whittemore Jr., J. Can. Ceram. Soc. 28 (1959) 43, cited in Ref. [93].

[34] M. Faucher, F. Cabannes, A.M. Anthony, B. Piriou, J. Simonato, Rev. Int. Hautes Temp. Refract. 7 (1970) 290.

[35] W.D. Kingery, J. Francl, R.L. Cobble, T. Vasilos, J. Am. Ceram. Soc. 37 (1954) 107.

[36] D.L. McElroy, J.P. Moore, P.H. Spindler, Oak Ridge National Laboratory Report ORNL-4429, 1968, p. 121.

[37] B. Schulz, High Temp.-High Press. 13 (1981) 649.

[38] S. Fukushima, T. Ohmichi, A. Maeda, H. Watanbe, J. Nucl. Mater. 105 (1982) 201.

[39] Armour Research Foundation ARF-Project No 6-025, Final Report, 1957, cited in Ref. [27].

[40] J.C. Weilbacher, High Temp.-High Press. 4 (1972) 431.

[41] W.R. DeBoskey, in: Proceedings of the Thorium Fuel Symposium, Gatlinburg, TN, 1962. TID-7650, book 2.

[42] M. Murabayashi, J. Nucl. Sci. Technol. 7 (1970) 559.

[43] J.H. Koenig, Rutgers Univ. NJ, Ceram. Research Sta. Progr. Report, Vol. 2, 1953, p. 1, cited in Ref. [27].

[44] J. Holzer, G. McCarthy, JCPDS-File Card No. 42-1462.

[45] Y.S. Touloukian, R.K. Kirby, R.E. Taylor, T.Y.R. Lee,

Thermal Expansion. Nonmetallic Solids (IFI/Plenum, New York, 1970).
[46] W.A. Lambertson, M.H. Mueller, F.H. Gunzel, J. Am. Ceram. Soc. 36 (1953) 397.
[47] E. Slowinski, N. Elliott, Acta Crystallogr. 5 (1952) 768.
[48] M. Kanno, S. Kokubo, H. Furuya, J. Nucl. Sci. Technol. 19 (1982) 956.
[49] W. Trzebiatowski, P.W. Selwood, J. Am. Chem. Soc. 72 (1950) 4504.
[50] J.A. Christensen, General Electric Report HW-76559, 1962, p 11.7.
[51] R.E. Latta, E.C. Duderstadt, R.E. Fryxell, J. Nucl. Mater. 35 (1970) 347.
[52] D.F. Fischer, J.K. Fink, L. Leibowitz, J. Belle, J. Nucl. Mater. 118 (1983) 342.
[53] T.B. Lindemer, T.M. Besmann, J. Nucl. Mater. 130 (1985) 473.
[54] R.P.C. Schram, E.H.P. Cordfunke, to be published.
[55] A. Nakamura, T. Fujino, J. Nucl. Mater. 140 (1986) 113.
[56] A. Nakamura, T. Fujino, J. Nucl. Mater. 149 (1987) 80.
[57] T. Matsui, K. Naito, J. Nucl. Sci. Technol. 12 (1975) 250.
[58] K. Park, D.R. Olander, High. Temp. Sci. 29 (1990) 203.
[59] T.M. Besmann, T.B. Lindemer, J. Nucl. Mater. 130 (1985) 489–504.
[60] W. Breitung, KFK 2663, Kernforchungszentrum Karlsruhe Report, 1976.
[61] K. Park, D.R. Olander, J. Nucl. Mater. 187 (1992) 89.
[62] W.-E. Wang, D.R. Olander, T.B. Lindemer, J. Nucl. Mater. 211 (1994) 85.
[63] B.T.M. Willis, Nature 197 (1963) 755.
[64] A.D. Murray, B.T.M. Willis, J. Solid State Chem. 84 (1990) 52.
[65] R.M. Berman, T.S. Tully, J. Belle, I. Goldberg, Westinghouse Report WAPD-TM-908, 1972.
[66] D.C. Jacobs, Westinghouse Report WAPD-TM-758, 1969.
[67] D.C. Jacobs, Westinghouse Report WAPD-TM-901, 1970.
[68] J. Matolich, V.W. Storhok, Battelle Memorial Institute Report BMI-RX-10274, 1970.
[69] M. Murabayashi, S. Namba, Y. Takahashi, T. Mukaibo, J. Nucl. Sci. Technol. 6 (1969) 128.
[70] P. Srirama Murti, C.K. Mathews, J. Phys. D24 (1991) 2202.
[71] P. Srirama Murti, C.K. Mathews, High Temp.-High Press. 22 (1990) 379.
[72] P.G. Lucuta, H.J. Matzke, R.A. Verrall, J. Nucl. Mater. 217 (1994) 279.
[73] S. Fukushima, T. Ohmichi, M. Handa, J. Less-Common Met. 121 (1986) 631, and references cited in this paper.
[74] S. Fukushima, T. Ohmichi, A. Maeda, H. Watanbe, J. Nucl. Mater. 102 (1981) 30.
[75] C.P. Kempter, R.O. Elliot, J. Chem. Phys. 30 (1959) 1524.
[76] E.D. Lynch, R.J. Beals, Argonne National Laboratory, Annual report for 1962, ANL-6677, 1962, p. 101.
[77] D.N. Turner, P.D. Smith, Australian Atomic Energy Commission report AAEC/E183, 1967.
[78] A.C. Momin, E.B. Mirza, M.D. Mathews, J. Nucl. Mater. 185 (1991) 308.
[79] R.M. Powers, H. Shapiro, Quarterly Technical Progress Report, Sylvania Corning Nuclear Corp. SCNC-301, 1959.
[80] D.G. Martin, J. Nucl. Mater. 152 (1988) 94.
[81] M.D. Freshley, H.M. Mattys, General Electric Report HW-76559, 1962, p. 11.6.
[82] HW-76300, Quarterly report Ceramics research and development operation, General Electric, 1962.
[83] U. Basak, A.K. Sengupta, C. Ganguly, J. Mater. Sci. Lett. 8 (1989) 449.
[84] A.T. Jeffs, Trans. Am. Nucl. Soc. 11 (1968) 497.
[85] A.T. Jeffs, Atomic Energy of Canada Limited Report AECL-3294, 1968.
[86] I.J. Hastings, T.J. Carter, G. MacGillivray, R.D. MacDonald, J. Judah, Proc. Canadian Nuclear Society, 6th Annual Conf., 1985, p. 6.26.
[87] K. Anantharaman, Bhabha Atomic Research Centre Report, BARC-1532, 1990, p. 41.
[88] O. Ruff, F. Ebert, H. Woitinek, Z. Anorg. Allgem. Chem. 180 (1929) 252.
[89] H. Wartenberg, H.J. Reusch, Z. Anorg. Allgem. Chem. 208 (1932) 369.
[90] G.A. Geach, M.E. Harper, Metallurgia 47 (1953) 269.
[91] R. Benz, J. Nucl. Mater. 29 (1969) 43.
[92] T.D. Chikalle, C.E. McNeilly, J.L. Bates, J.J. Rasmussen, Colloq. Int. Centre Nat. Rech. Sci. N 205 (1972) 351.
[93] P.T.B. Shaffer, Handbooks of High-Temperature Materials, Vol. 1 (Plenum, New York, 1963) p. 308.
[94] M. Adams, J. Am. Ceram. Soc. 37 (1954) 74.
[95] W.G. Bradshaw, C.O. Mathews, Report LMSD-2466, 1958, cited in Ref. [93].
[96] J.P. Moore, R.S. Graves, T.G. Kollie, D.L. McElroy, Oak Ridge National Laboratory Report ORNL-4121, 1967.
[97] V.P. Glushko, L.V. Gurvich, G.A. Bergman, I.V. Veyts, V.A. Medvedev, G.A. Khachkuruzov, V.S. Yungman, Termodinamicheskie Svoistva Individual'nykh Veshchestv. (Nauka, Moscow, 1982).
[98] E.H.P. Cordfunke, R.J.M. Konings, Thermochemical Data for Reactor Materials and Fission Products (Elsevier, Amsterdam, 1990).
[99] J.S. Anderson, D.N. Edgington, L.E.J. Roberts, E. Wait, J. Chem. Soc. (1954) 3324.
[100] L.E.J. Roberts, L.E. Russell, A.G. Adwick, A.J. Walter, M.H. Rand, 2nd Geneva Conf. on Peaceful Uses of Atomic Energy, Vol. 28, 1958, p. 215.
[101] S. Aronson, J.C. Clayton, J. Chem. Phys. 32 (1960) 749.
[102] S. Tanaka, E. Kimura, A. Yamaguchi, J. Moriyama, J. Jpn. Inst. Met. 36 (1972) 633.
[103] M. Ugajin, J. Nucl. Mater. 110 (1982) 140.
[104] M. Ugajin, T. Shiratori, K. Shiba, J. Nucl. Mater. 116 (1983) 172.
[105] M. Ugajin, J. Nucl. Sci. Technol. 20 (1983) 228.
[106] T. Matsui, K. Naito, J. Nucl. Mater. 132 (1985) 212.
[107] W.D. Kingery, J. Am. Ceram. Soc. 42 (1959) 617.
[108] S.V.K. Rao, J. Nucl. Mater. 12 (1964) 323.
[109] S.V.K. Rao, Atomic Energy of Canada Limited Report AECL-1785, 1963.
[110] E.N. Harbinson, R.J. Walker, Trans. Am. Nucl. Soc. 9 (1966) 26.
[111] C. Ferro, C. Patimo, C. Piconi, J. Nucl. Mater. 43 (1972) 273.
[112] Program of Research and Development on the Thorium Utilization in PWR's, Final report (1979–1988), Kernforchungsanlage Jülich Report, Jül-Spez-488, 1988.